

# IMPLICIT STRESS INTEGRATION FOR ELASTIC-PLASTIC DEFORMATION OF VON MISES MATERIAL WITH MIXED HARDENING

*M. Kojić*

(Received 17.12.1993)

## 1. Introduction

Implicit stress integration in the incremental analysis of the strain-driven problems has advantages with respect to other procedures [1]–[5]. The basic idea of reducing the problem of stress integration to solution of one nonlinear equation is presented in [6] for elastic-plastic and/or creep deformation of metals, and implemented in [7] to shell and beam analysis. That computation procedure is applied to the Cam-clay material [8] and further generalized into a governing parameter method (GPM) in [1]. Also, this procedure has been implemented to the various material models, including anisotropic metal plasticity [9] and large strains [2].

In this paper we first outline the basic concept of the GPM and then in section 3 derive the governing relations for stress integration (for general 3-D, plane stress/shell and beam conditions) and for the elastic-plastic matrix in case of the isotropic von Mises plasticity with mixed hardening. In section 4 we give two numerical examples, and, finally, in section 5 we present some concluding remarks.

## 2. The Governing Parameter Method

As described in [1], the governing parameter method consists in the following. We suppose that the known quantities at a material point are

$${}^t\sigma, {}^t\epsilon, {}^t\epsilon^{IN}, {}^t\beta, {}^{t+\Delta t}\epsilon \quad (2.1)$$

where  ${}^t\sigma$  are stress,  ${}^t\epsilon$  – strains,  ${}^t\epsilon^{IN}$  – inelastic strain,  ${}^t\beta$  – internal variables, at start of time step; and  ${}^{t+\Delta t}\epsilon$  are strains at end of time step. The unknowns to be determined are

$${}^{t+\Delta t}\sigma, {}^{t+\Delta t}\epsilon^{IN}, {}^{t+\Delta t}\beta \quad (2.2)$$

We use the left superscript to denote that a quantity corresponds to start or to end of time (load) step. We suppose that it is possible to express the

unknowns in terms of one governing parameter  $p$ . Then, we form a governing scalar nonlinear equation

$$f(p) = 0 \quad (2.3)$$

whose solution is  ${}^{t+\Delta t}p$ . With the governing parameter  ${}^{t+\Delta t}p$  calculated, we determine the unknowns (2.2).

A very important task in practical applications is to determine the true-tangent constitutive tensor corresponding to end of time step. Following the GPM we have

$${}^{t+\Delta t}\mathbf{C} = \frac{\partial {}^{t+\Delta t}\underline{\underline{\sigma}}}{\partial {}^{t+\Delta t}\underline{\underline{e}}} = \frac{\partial {}^{t+\Delta t}\underline{\underline{\sigma}}}{\partial {}^{t+\Delta t}p} \frac{\partial {}^{t+\Delta t}p}{\partial {}^{t+\Delta t}\underline{\underline{e}}} \quad (2.4)$$

Derivatives  $\partial {}^{t+\Delta t}p / \partial {}^{t+\Delta t}\underline{\underline{e}}$  can be calculated by differentiation of the governing equation (2.3) with respect to strains  ${}^{t+\Delta t}\underline{\underline{e}}$ , i.e.

$$\begin{aligned} \frac{df}{d{}^{t+\Delta t}\underline{\underline{e}}} = & \left( \frac{\partial f}{\partial {}^{t+\Delta t}\underline{\underline{\sigma}}} \frac{\partial {}^{t+\Delta t}\underline{\underline{\sigma}}}{\partial {}^{t+\Delta t}p} + \frac{\partial f}{\partial {}^{t+\Delta t}\underline{\underline{e}}^{\text{IN}}} \frac{\partial {}^{t+\Delta t}\underline{\underline{e}}^{\text{IN}}}{\partial {}^{t+\Delta t}p} + \right. \\ & \left. \frac{\partial f}{\partial {}^{t+\Delta t}\underline{\underline{\beta}}} \frac{\partial {}^{t+\Delta t}\underline{\underline{\beta}}}{\partial {}^{t+\Delta t}p} \right) \frac{\partial {}^{t+\Delta t}p}{\partial {}^{t+\Delta t}\underline{\underline{e}}} + \frac{\partial f}{\partial {}^{t+\Delta t}\underline{\underline{e}}} = 0 \end{aligned} \quad (2.5)$$

We use derivatives with respect to tensors, with the meaning, for example,  $\partial / \partial {}^{t+\Delta t}\underline{\underline{e}} = \partial / \partial e_{km} \mathbf{i}_k \mathbf{i}_m$ , where  $\mathbf{i}_k$  and  $\mathbf{i}_m$  are the base vectors in a Cartesian coordinate system. In the expression for  ${}^{t+\Delta t}\mathbf{C}$  we will employ the one-index notation for stress and strains; hence, in componental form we write the fourth-order tensor  ${}^{t+\Delta t}\mathbf{C}$  in (2.4) as the two-dimensional matrix,

$${}^{t+\Delta t}C_{ij} = \frac{\partial {}^{t+\Delta t}\sigma_i}{\partial {}^{t+\Delta t}e_j} \quad (2.6)$$

### 3. Von Mises Plasticity Model with Mixed Hardening

Here we apply the GPM to the von Mises material with mixed hardening. The main characteristics of this model are shown in Fig. 1. Two yield surfaces corresponding to start and end of time (load) step show that the yield surface translates and changes the size in the deviatoric plane. The yield curve which represents the relation between the size of the yield surface  $\hat{\sigma}$  and the isotropic part of the effective plastic strain  $\bar{e}^p = M\bar{e}^p$ , where  $M$  is the mixed hardening parameter ( $0 \leq M \leq 1$ ,  $M = 0$  - kinematic hardening,  $M = 1$  - isotropic hardening), is shown in the figure.

We start with a general 3-D deformation. The constitutive relations for the mean stress  ${}^{t+\Delta t}\sigma_m$  and for deviatoric stress  ${}^{t+\Delta t}\mathbf{S}$  at the end of time step are

$${}^{t+\Delta t}\sigma_m = c_m {}^{t+\Delta t}e_m \quad \text{no sum on } m \quad (3.1)$$

$${}^{t+\Delta t}\mathbf{S} = 2G ({}^{t+\Delta t}\underline{\underline{e}}'' - \Delta e^p) \quad (3.2)$$

where  $c_m = 3K$  ( $K$  is the bulk modulus),  $G$  is the shear modulus,  ${}^{t+\Delta t}e_m = {}^{t+\Delta t}e_{ii}/3$  is the mean strain,  $\Delta e^p$  is increment of plastic strain, and  ${}^{t+\Delta t}e''$  is

$${}^{t+\Delta t}e'' = {}^{t+\Delta t}e' - {}^te^p \tag{3.3}$$

Here  ${}^{t+\Delta t}e'$  is deviatoric strain, and  ${}^te^p$  - plastic strain at start of time step. In the above relations the incompressibility of plastic deformation

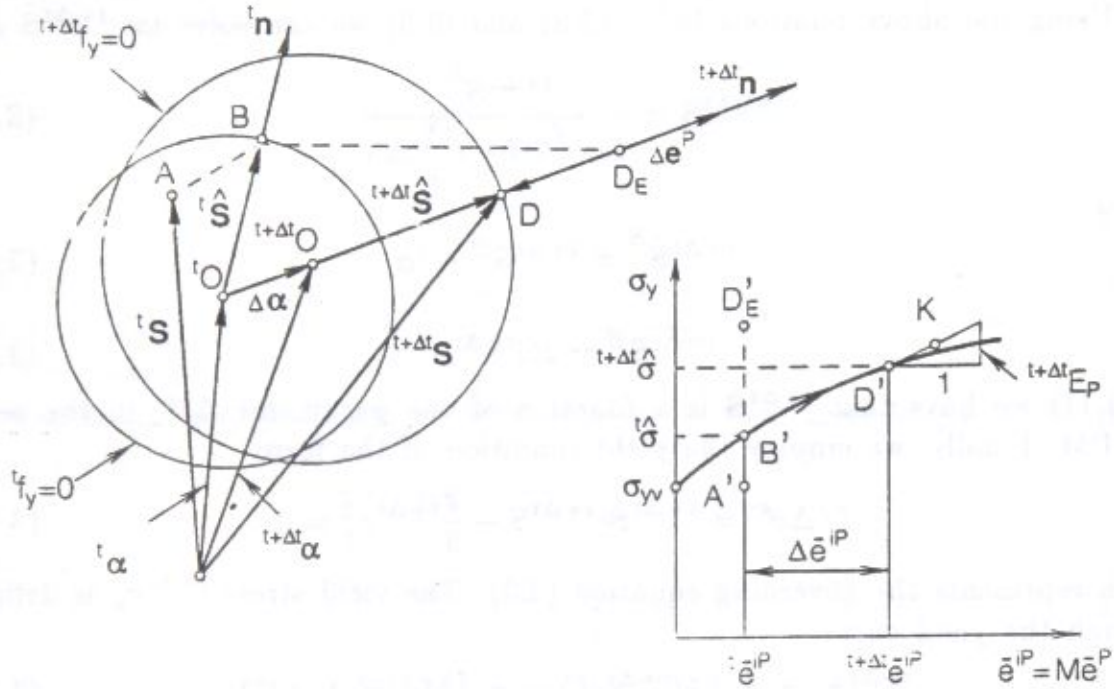


Figure 1. Stress states and the yield surfaces at start and at end of time step, in deviatoric plane and on the yield curve

is taken into account. Further, we use the flow rule, therefore we have

$$\Delta e^p = \Delta \lambda {}^{t+\Delta t} \hat{S} \tag{3.4}$$

where  $\Delta \lambda$  is a positive scalar, which can be related to increment of effective plastic strain as

$$\Delta \lambda = \frac{3}{2} \frac{\Delta \bar{e}^p}{{}^{t+\Delta t} \hat{\sigma}} \tag{3.5}$$

and  ${}^{t+\Delta t} \hat{S}$  is the radius of the yield surface. Definition of  $\Delta \bar{e}^p$  and  ${}^{t+\Delta t} \hat{\sigma}$  are as follows

$$\Delta \bar{e}^p = \left( \frac{2}{3} \Delta e^p \cdot \Delta e^p \right)^{1/2} = \left( \frac{2}{3} \Delta e_{ij}^p \Delta e_{ij}^p \right)^{1/2} \tag{3.6}$$

$${}^{t+\Delta t} \hat{\sigma} = \left( \frac{3}{2} {}^{t+\Delta t} \hat{S} \cdot {}^{t+\Delta t} \hat{S} \right)^{1/2} \tag{3.7}$$

The yield condition at end of time step can be expressed in the form

$${}^{t+\Delta t} S = \underline{{}^t \alpha} + \underline{\Delta \alpha} + {}^{t+\Delta t} \hat{S} \tag{3.8}$$

For increment of the back stress  $\underline{\alpha}$  we use the constitutive relation

$$\Delta \underline{\alpha} = \hat{C} \Delta e^p = \hat{C} \Delta \lambda {}^{t+\Delta t} \hat{S} \quad (3.9)$$

where

$$\hat{C} = \frac{2}{3} (1 - M) \bar{E}_p \quad (3.10)$$

is the modulus expressed in terms of a weighted plastic modulus for time step  $\bar{E}_p$ .

Using the above relations (3.2), (3.8) and (3.9) we can solve for  ${}^{t+\Delta t} \hat{S}$  as

$${}^{t+\Delta t} \hat{S} = \frac{{}^{t+\Delta t} \hat{S}^E}{1 + (2G + \hat{C}) \Delta \lambda} \quad (3.11)$$

where

$${}^{t+\Delta t} \hat{S}^E = {}^{t+\Delta t} S^E - {}^t \alpha \quad (3.12)$$

and

$${}^{t+\Delta t} S^E = 2G {}^{t+\Delta t} e'' \quad (3.13)$$

In (3.11) we have that  ${}^{t+\Delta t} \hat{S}$  is a function of one parameter  $\Delta \bar{e}^p$ , in the sense of GPM. Finally, we employ the yield condition of the form

$$f(\Delta \bar{e}^p) = {}^{t+\Delta t} \hat{S} \cdot {}^{t+\Delta t} \hat{S} - \frac{2}{3} {}^{t+\Delta t} \hat{\sigma}_y^2 = 0 \quad (3.14)$$

which represents the governing equation (2.3). The yield stress  ${}^{t+\Delta t} \hat{\sigma}_y$  is defined through the yield curve

$${}^{t+\Delta t} \hat{\sigma}_y = \sigma_y (M {}^{t+\Delta t} \bar{e}^p) = \sigma_y [M ({}^t \bar{e}^p + \Delta \bar{e}^p)] \quad (3.15)$$

The computational procedure is as follows: we solve (3.14) for  $\Delta \bar{e}^p$  using (3.5), (3.15) and (3.11), then from (3.8) and (3.9) we calculate  ${}^{t+\Delta t} \hat{S}$  and obtain stresses  ${}^{t+\Delta t} \underline{\sigma}$  by adding the mean stress  ${}^{t+\Delta t} \sigma_m$  from (3.1); increments of plastic strains follow from (3.4). As it can be seen, the stress integration is reduced to solution of the scalar equation (3.14).

Further, we briefly present the solution procedure for the plane stress/shell conditions. If  $z$  is the axis for which the normal stress is equal to zero (normal to the midsurface in case of shell), i.e.

$$\sigma_{zz} = 0 \quad (3.16)$$

than we need to correct the constitutive relations (3.2) in order to satisfy the condition (3.16). Practically, we correct the elastic constitutive matrix  $C^E$  and then, instead of uncoupled relations (3.2), we obtain expressions for the in-plane components  ${}^{t+\Delta t} S_{xx}$  and  ${}^{t+\Delta t} S_{yy}$  in the form

$${}^{t+\Delta t} S_{xx} = {}^{t+\Delta t} S_{xx}^E - \Delta \lambda \left( \bar{C}_1^{E,t+\Delta t} \hat{S}_{xx} + \bar{C}_2^{E,t+\Delta t} \hat{S}_{yy} \right) \quad (3.17)$$

$${}^{t+\Delta t} S_{yy} = {}^{t+\Delta t} S_{yy}^E - \Delta \lambda \left( \bar{C}_2^{E,t+\Delta t} \hat{S}_{xx} + \bar{C}_1^{E,t+\Delta t} \hat{S}_{yy} \right)$$

where  $\bar{C}_1^E$  and  $\bar{C}_2^E$  are elastic constants expressible in terms of the Young's modulus  $E$  and Poisson's ratio  $\nu$ . These relations, together with the yield condition (3.8) can be solved with respect to  ${}^{t+\Delta t}\hat{S}_{xx}$  and  ${}^{t+\Delta t}\hat{S}_{yy}$  [2]. The third component  ${}^{t+\Delta t}\hat{S}_{zz}$  follows from the deviatoric character of  ${}^{t+\Delta t}\hat{S}$ , while the shear components of the radius  ${}^{t+\Delta t}\hat{S}$  are given by (3.11). Under these conditions we form again the governing equation (3.14) to solve for  $\Delta e^p$ , and calculate stresses  ${}^{t+\Delta t}\underline{\sigma}$ , increments  $\Delta e^p$  and  $\Delta \underline{\alpha}$  in a way analogous to the above described for 3-D deformation.

In case of beam deformation we only have one nonzero normal stress  $\sigma_{xx}$  in the beam axis direction. Then the constitutive relation for  ${}^{t+\Delta t}S_{xx}$  is

$${}^{t+\Delta t}S_{xx} = \frac{2}{3}{}^{t+\Delta t}\sigma_{xx} = \frac{2}{3}E \left( {}^{t+\Delta t}e''_{xx} - \Delta e^p_{xx} \right) \quad (3.18)$$

where  ${}^{t+\Delta t}e''_{xx} = {}^{t+\Delta t}e_{xx} - {}^te^p_{xx}$ . Also,  ${}^{t+\Delta t}S_{yy} = {}^{t+\Delta t}S_{zz} = -1/2{}^{t+\Delta t}S_{xx}$ . With these conditions we can again form the governing equation (3.14) and proceed in a way analogous to the 3-D procedure.

The elastic-plastic matrix  ${}^{t+\Delta t}C^{EP}$  can be written, according to (2.6), (3.1) and (3.2), as

$${}^{t+\Delta t}C^{EP}_{ij} = {}^{t+\Delta t}C^m_{ij} + {}^{t+\Delta t}C'_{ij} \quad (3.19)$$

where

$${}^{t+\Delta t}C^m_{ij} = \frac{1}{3}c_m \delta_{ij} \quad (3.20)$$

and

$${}^{t+\Delta t}C'_{ij} = \frac{\partial {}^{t+\Delta t}S_i}{\partial {}^{t+\Delta t}e_j} \quad (3.21)$$

with  $\delta_{ij}$  being Kronecker delta symbol. The coefficients  ${}^{t+\Delta t}C'_{ij}$  can be expressed in terms of derivatives  ${}^{t+\Delta t}\bar{C}'_{ij} = \partial {}^{t+\Delta t}S_i / \partial {}^{t+\Delta t}e''_j$  using (3.3) and the condition that the shear components are  ${}^{t+\Delta t}e''_k = 1/2{}^{t+\Delta t}\gamma_k$  (in  ${}^{t+\Delta t}C^{EP}$  derivatives of stresses are taken with respect to shear engineering strain components  ${}^{t+\Delta t}\gamma_k$ ). Therefore, we have that [1]

$$\left[ \frac{\partial {}^{t+\Delta t}e''_j}{\partial {}^{t+\Delta t}e_j} \right] = \frac{1}{3} \begin{bmatrix} 2 & -1 & -1 \\ -1 & 2 & -1 \\ -1 & -1 & 2 \end{bmatrix} \quad i, j = 1, 2, 3 \quad (3.22)$$

while

$$\frac{\partial {}^{t+\Delta t}e''_k}{\partial {}^{t+\Delta t}\gamma_s} = \frac{1}{2}\delta_{ks} \quad (3.23)$$

The problem of calculation of  ${}^{t+\Delta t}C^{EP}$  is reduced to finding derivatives  $\bar{C}'_{ij}$ . From (3.2) and (3.4) follows

$$\bar{C}'_{ij} = \frac{\partial {}^{t+\Delta t}S_i}{\partial {}^{t+\Delta t}e''_j} = \bar{C}'^E_{ij} - 2G \left( {}^{t+\Delta t}\hat{S}_i \Delta \lambda_j + \Delta \lambda {}^{t+\Delta t}\hat{S}_{i,j} \right) \quad (3.24)$$

where  $\partial/\partial^{t+\Delta t} e_j'' \equiv \cdot_j$  is used. The coefficients  $\bar{C}_{ij}^E$  are  $\bar{C}_{ij}^E = 2G \delta_{ij}$ . By employing (3.5) and (3.11) we obtain

$$\Delta \lambda_{,j} = b_1 \Delta \bar{e}_{,j}^p \quad (3.25)$$

$${}^{t+\Delta t} \hat{S}_{i,j} = a_\lambda \delta_{ij} - b_\lambda {}^{t+\Delta t} \hat{S}_i \Delta \bar{e}_{,j}^p$$

where

$$b_1 = \frac{1}{{}^{t+\Delta t} \hat{\sigma}} \left( \frac{3}{2} - \Delta \lambda M {}^{t+\Delta t} \hat{E}_p \right)$$

$$a_\lambda = \frac{2G}{1 + \Delta \lambda (2G + \hat{C})} \quad (3.26)$$

$$b_\lambda = \frac{b_1 (2G + \hat{C}) + \Delta \lambda b_2}{1 + \Delta \lambda (2G + \hat{C})}$$

$$b_2 = \frac{2}{3} (1 - M) \frac{\partial \bar{E}_p}{\partial (\Delta \bar{e}^p)}$$

and  ${}^{t+\Delta t} \hat{E} = \partial^{t+\Delta t} \hat{\sigma} / \partial^{t+\Delta t} \bar{e}^p$ . According to the GPM outlined in section 2, we obtain derivatives  $\Delta \bar{e}_{,j}^p$  by differentiation of the governing equation (3.14) with respect to  ${}^{t+\Delta t} e_j''$ . Then we obtain

$$\Delta \bar{e}_{,j}^p = \frac{a_\lambda}{b_p} {}^{t+\Delta t} \hat{S}'_j \quad (3.27)$$

where

$$b_p = b_\lambda b_3 + \frac{2}{3} M {}^{t+\Delta t} \hat{\sigma}_y {}^{t+\Delta t} \hat{E}_p \quad (3.28)$$

$$b_3 = {}^{t+\Delta t} \hat{S}_i {}^{t+\Delta t} \hat{S}'_i$$

and

$${}^{t+\Delta t} \hat{S}'_i = {}^{t+\Delta t} \hat{S}_i, \quad i = 1, 2, 3 \quad (3.29)$$

$${}^{t+\Delta t} \hat{S}'_i = 2 {}^{t+\Delta t} \hat{S}_i, \quad i = 4, 5, 6$$

Finally, substituting (3.27) into (3.25) and then into (3.24), we obtain the following expression for  ${}^{t+\Delta t} \hat{S}_{i,j}$  suitable for application

$$\bar{C}'_{ij} = 2G (1 - \Delta \lambda a_\lambda) \delta_{ij} - c_\lambda {}^{t+\Delta t} \hat{S}_i {}^{t+\Delta t} \hat{S}'_j \quad (3.30)$$

where

$$c_\lambda = \frac{2Ga_\lambda}{b_p} (b_1 - \Delta\lambda b_\lambda) \tag{3.31}$$

The above derivations are given for 3-D deformation. For shell and beam conditions we need to perform the corresponding static condensations.

#### 4. Numerical Examples

Here we present two examples characteristic for illustration of the above described computational procedure. Other interesting examples are given in [2].

##### (a) A Plate Loaded by In-Plane Stresses

A plate material element is loaded by given stresses. Geometrical, loading and material data are given in Fig. 2(a). Considering that stress/strain state is uniform within the element, determine displacements for isotropic, kinematic and mixed ( $M = 0.5$ ) hardening conditions. Use  ${}^tE_p$  and  ${}^{t+\Delta t}E_p$  for  $\bar{E}_p$  in (3.10) and employ two steps in the analysis.

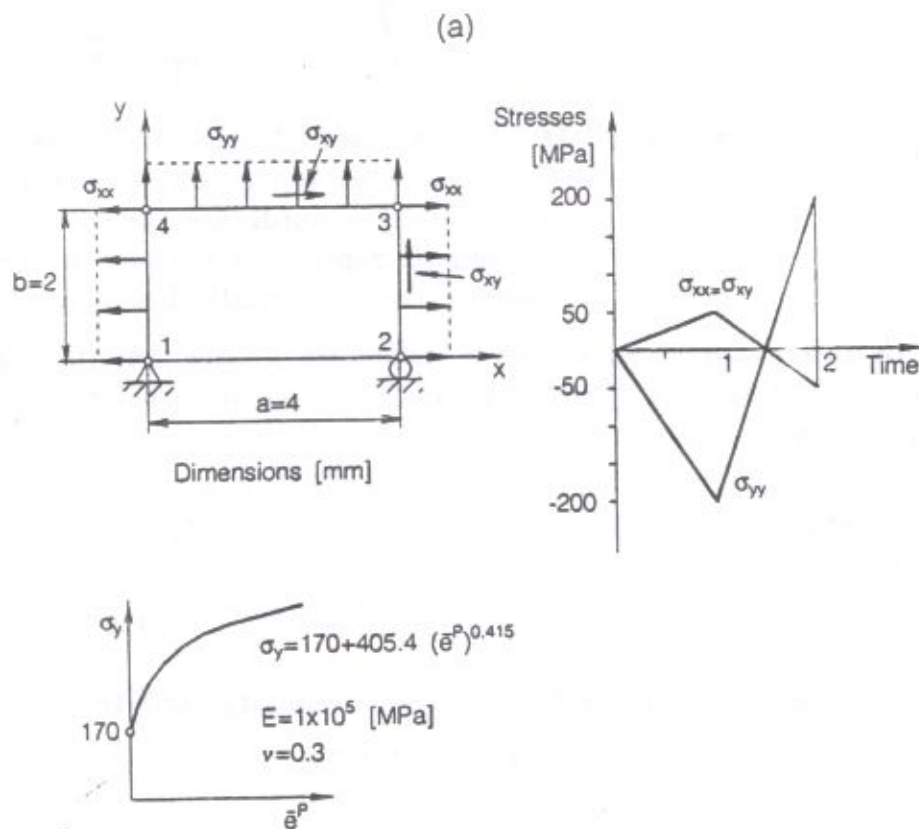


Figure 2. Plate element loaded by given stresses

(a) Boundary conditions, loading and material data

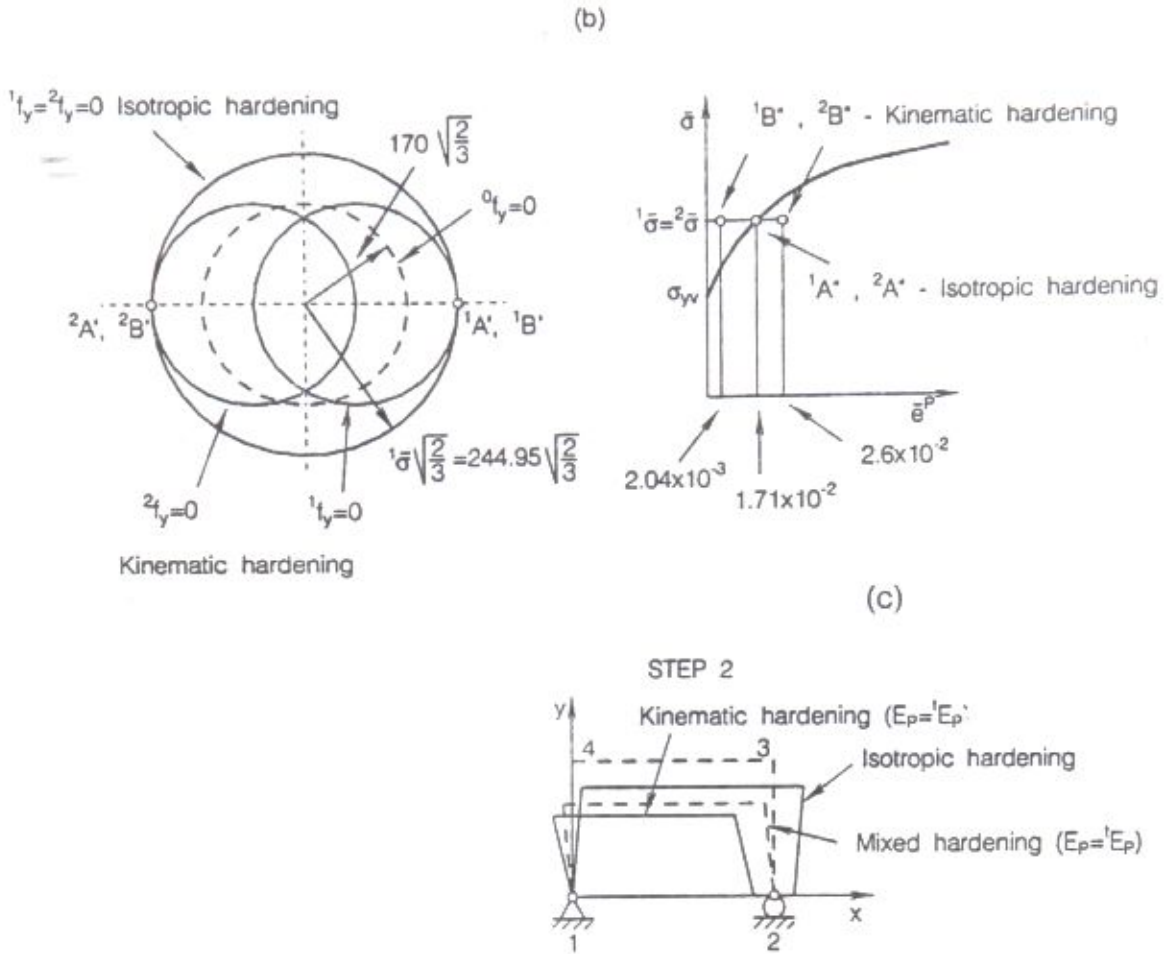


Figure 2. Plate element loaded by given stresses

- (b) Yield surfaces and representative points in stress space and in coordinate system  $\bar{\sigma}$ ,  $\bar{e}^P$
- (c) Schematic representation of deformed shapes for isotropic and kinematic hardening, step 2

With this example we illustrate difference in the material response due to various assumptions for hardening, and also we demonstrate influence of the modulus  $\bar{E}_p$  in (3.10) on results.

The plasticity calculations are as described in section 3. We note that in case of kinematic hardening the condition  ${}^{t+\Delta t}\hat{\sigma}_y = \sigma_{yv}$  is used in (3.14). The strains are calculated as

$${}^{t+\Delta t}e_{ij} = \frac{{}^{t+\Delta t}S_{ij}}{2G} + \frac{{}^{t+\Delta t}\sigma_m \delta_{ij}}{c_m} + {}^{t+\Delta t}e_{ij}^p \quad (4.1)$$

and displacements, according to the given boundary conditions, are

$$u_x = e_{xx} x + \gamma_{xy} y \quad (4.2)$$

$$u_y = e_{yy} y$$

Some of the results are given in Table 1, where  $\bar{\sigma}$  is the effective stress for isotropic hardening obtained from (3.7) with  ${}^{t+\Delta t}\mathbf{S}$  used for  ${}^{t+\Delta t}\hat{\mathbf{S}}$ .



Table 1. Results for isotropic, kinematic and mixed hardening

step 1/step 2		Isotropic hardening			
$\bar{\sigma}, \bar{\epsilon}^p, \Delta\lambda$	$0.2449 \times 10^3$	$0.1718 \times 10^{-1}$	$0.1048 \times 10^{-3}$		
	$0.2449 \times 10^3$	$0.1718 \times 10^{-1}$	0.		
$\epsilon_{xx}^p, \epsilon_{yy}^p, \epsilon_{zz}^p, \gamma_{xy}^p$	$0.1048 \times 10^{-1}$	$-0.1572 \times 10^{-1}$	$0.5241 \times 10^{-2}$	$0.1048 \times 10^{-1}$	
	$0.1048 \times 10^{-1}$	$-0.1572 \times 10^{-1}$	$0.5241 \times 10^{-2}$	$0.1048 \times 10^{-1}$	
$U_{x2}, U_{x3}, U_{x4}$ $U_{y3} = U_{y4}$	$0.4633 \times 10^{-1}$	$0.6990 \times 10^{-1}$	$0.2357 \times 10^{-1}$	$-0.3575 \times 10^{-1}$	
	$0.3753 \times 10^{-1}$	$0.5590 \times 10^{-1}$	$0.1837 \times 10^{-1}$	$-0.2715 \times 10^{-1}$	
Kinematic hardening $E_p = {}^t E_p$					
$\bar{\sigma}, \bar{\epsilon}^p, \Delta\lambda$	$0.1700 \times 10^3$	$0.2036 \times 10^{-2}$	$0.1797 \times 10^{-4}$		
	$0.1700 \times 10^3$	$0.2578 \times 10^{-1}$	$0.2095 \times 10^{-3}$		
$\epsilon_{xx}^p, \epsilon_{yy}^p, \epsilon_{zz}^p, \gamma_{xy}^p$	$0.1247 \times 10^{-2}$	$-0.1870 \times 10^{-2}$	$0.6235 \times 10^{-3}$	$0.1247 \times 10^{-2}$	
	$-0.1329 \times 10^{-1}$	$0.1994 \times 10^{-1}$	$-0.6646 \times 10^{-2}$	$-0.1329 \times 10^{-1}$	
$U_{x2}, U_{x3}, U_{x4}$ $U_{y3} = U_{y4}$	$0.9388 \times 10^{-2}$	$0.1448 \times 10^{-1}$	$-0.5094 \times 10^{-2}$	$-0.8041 \times 10^{-2}$	
	$-0.5757 \times 10^{-1}$	$-0.8675 \times 10^{-1}$	$-0.2918 \times 10^{-1}$	$0.4418 \times 10^{-1}$	
Kinematic hardening $E_p = {}^{t+\Delta t} E_p$					
$\bar{\sigma}, \bar{\epsilon}^p, \Delta\lambda$	$0.1700 \times 10^3$	$0.1425 \times 10^0$	$0.1257 \times 10^{-2}$		
	$0.1700 \times 10^3$	$0.1069 \times 10^1$	$0.8174 \times 10^{-2}$		
$\epsilon_{xx}^p, \epsilon_{yy}^p, \epsilon_{zz}^p, \gamma_{xy}^p$	$0.8726 \times 10^{-1}$	$-0.1309 \times 10^0$	$0.4363 \times 10^{-1}$	$0.8726 \times 10^{-1}$	
	$-0.4800 \times 10^0$	$0.7200 \times 10^0$	$-0.2400 \times 10^0$	$-0.4800 \times 10^0$	
$U_{x2}, U_{x3}, U_{x4}$ $U_{y3} = U_{y4}$	$0.3534 \times 10^0$	$0.5306 \times 10^0$	$0.1771 \times 10^0$	$-0.2661 \times 10^0$	
	$-0.1924 \times 10^1$	$-0.2887 \times 10^1$	$-0.9626 \times 10^0$	$0.1444 \times 10^1$	
Mixed hardening $E_p = {}^{t+\Delta t} E_p$					
$\bar{\sigma}, \bar{\epsilon}^p, \Delta\lambda$	$0.2287 \times 10^3$	$0.1900 \times 10^{-1}$	$0.1246 \times 10^{-3}$		
	$0.2497 \times 10^3$	$0.3970 \times 10^{-1}$	$0.1243 \times 10^{-3}$		
$\epsilon_{xx}^p, \epsilon_{yy}^p, \epsilon_{zz}^p, \gamma_{xy}^p$	$0.1164 \times 10^{-1}$	$-0.1746 \times 10^{-1}$	$0.5819 \times 10^{-2}$	$0.1164 \times 10^{-1}$	
	$-0.1033 \times 10^{-2}$	$0.1550 \times 10^{-2}$	$-0.5166 \times 10^{-3}$	$-0.1033 \times 10^{-2}$	
$U_{x2}, U_{x3}, U_{x4}$ $U_{y3} = U_{y4}$	$0.5095 \times 10^{-1}$	$0.7683 \times 10^{-1}$	$0.2588 \times 10^{-1}$	$-0.3921 \times 10^{-1}$	
	$-0.8533 \times 10^{-2}$	$-0.1320 \times 10^{-1}$	$-0.4666 \times 10^{-2}$	$0.7400 \times 10^{-2}$	

We note that in case of isotropic hardening there is no further plastic deformation in step 2, as can be seen from Fig. 2(b), where the yield surfaces and the stress points for steps 1 and 2 are shown. For kinematic hardening and  $E_p = {}^tE_p$  we have used  $\bar{e}^p = 1 \times 10^{-4}$ . The stress points and the yield surfaces for mixed hardening lie between those shown for isotropic and kinematic hardening. Difference in results due to use of  ${}^tE_p$  or  ${}^{t+\Delta t}E_p$  is shown in Table 1, for kinematic hardening. Finally, the calculated material response is drastically affected by the adopted assumption of hardening, for the reverse loading conditions. This is shown in Fig. 2(c).

(b) Plane Strain Element under Compression

A material element loaded by given forces is shown in Fig. 3 (a). Supposing plane strain conditions and uniform stress/strain state within the element, determine displacements of nodal points using two steps.

This example demonstrates applicability of the GPM to plane strain conditions and also the high convergence rate due to tangent elastic-plastic moduli.

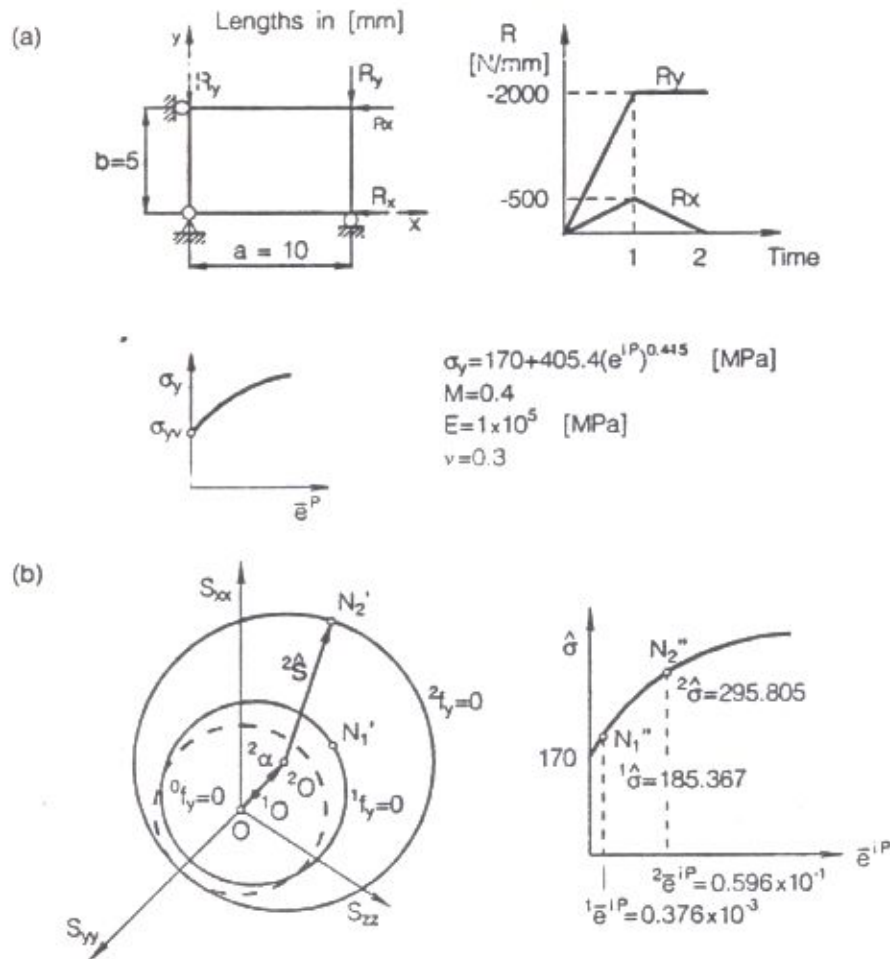


Figure 3. Plane strain element under compression

(a) Boundary and loading conditions

(b) Stress states in deviatoric plane and on the yield curve

According to the iterative solution scheme [1], we can form equilibrium equations of the form

$${}^{t+\Delta t}K_{xx}^{i-1} \Delta U_x^{(i)} - {}^{t+\Delta t}K_{xy}^{i-1} \Delta U_y^{(i)} = 2^{t+\Delta t}R_x - {}^{t+\Delta t}F_x^{i-1} \quad (4.3)$$

$${}^{t+\Delta t}K_{xy}^{i-1} \Delta U_x^{(i)} - {}^{t+\Delta t}K_{yy}^{i-1} \Delta U_y^{(i)} = 2^{t+\Delta t}R_y - {}^{t+\Delta t}F_y^{i-1}$$

where

$$\begin{aligned} {}^{t+\Delta t}K_{xx}^{i-1} &= \frac{b}{a} {}^{t+\Delta t}C_{xx}^{EP(i-1)} \\ {}^{t+\Delta t}K_{yy}^{i-1} &= \frac{a}{b} {}^{t+\Delta t}C_{yy}^{EP(i-1)} \\ {}^{t+\Delta t}K_{xy}^{i-1} &= {}^{t+\Delta t}C_{xy}^{EP(i-1)} \\ {}^{t+\Delta t}F_x^{i-1} &= b {}^{t+\Delta t}\sigma_{xx}^{(i-1)} \\ {}^{t+\Delta t}F_y^{i-1} &= a {}^{t+\Delta t}\sigma_{yy}^{(i-1)} \end{aligned} \quad (4.4)$$

Some of the calculated quantities are given in Table 2. In Table 3 are given unbalanced energies and unbalanced forces during iterations, showing the very high convergence rate.

Table 2. Some calculated quantities for the first and last iteration

Quantity	Step			
	1		2	
	Iteration (i)		Iteration (i)	
	1	5	1	6
$\Delta U_x^{(i)}$	$-0.260000 \times 10^{-2}$	$0.272220 \times 10^{-5}$	$0.751039 \times 10^{-1}$	$0.381160 \times 10^{-4}$
$\Delta U_y^{(i)}$	$-0.143000 \times 10^{-1}$	$-0.140338 \times 10^{-5}$	$-0.359014 \times 10^{-1}$	$-0.190572 \times 10^{-4}$
$U_x^{(i)}$	$-0.260000 \times 10^{-2}$	$0.399160 \times 10^{-2}$	$0.790955 \times 10^{-1}$	$0.130431 \times 10^1$
$U_y^{(i)}$	$-0.143000 \times 10^{-1}$	$-0.183875 \times 10^{-1}$	$-0.542889 \times 10^{-1}$	$-0.664091 \times 10^0$
$e_{xx}^{P(i)}$	$0.141397 \times 10^{-3}$	$0.395828 \times 10^{-3}$	$0.852846 \times 10^{-3}$	$0.767859 \times 10^{-3}$
$\sigma_{xx}^{(i)}$	$-0.208158 \times 10^3$	$-0.200000 \times 10^3$	$-0.119805 \times 10^3$	$-0.105990 \times 10^{-7}$
$\sigma_{yy}^{(i)}$	$-0.380966 \times 10^3$	$-0.400000 \times 10^3$	$-0.381557 \times 10^3$	$-0.400000 \times 10^3$
$\sigma_{xz}^{(i)}$	$-0.190877 \times 10^3$	$-0.219583 \times 10^3$	$-0.235693 \times 10^3$	$-0.196786 \times 10^3$
$\alpha_{xx}^{(i)}$	$0.917164 \times 10^0$	$0.214511 \times 10^1$	$0.926790 \times 10^1$	$0.283936 \times 10^2$
$\alpha_{yy}^{(i)}$	$-0.214005 \times 10^1$	$-0.371631 \times 10^1$	$-0.113238 \times 10^2$	$-0.300410 \times 10^2$
$\phi^{(i)}$	$0.178844 \times 10^3$	$0.185367 \times 10^3$	$0.209190 \times 10^3$	$0.295805 \times 10^3$
$\bar{e}^{P(i)}$	$0.248285 \times 10^{-3}$	$0.939954 \times 10^{-3}$	$0.897115 \times 10^{-2}$	$0.149073 \times 10^0$

Table 3. Unbalanced force and unbalanced energy during iteration

Iteration	Step 1		Step 2	
	$\ \Delta F^{(i)}\ /F_{ref}$	$\Delta E^{(i)}/\Delta E^{(0)}$	$\ \Delta F^{(i)}\ /F_{ref}$	$\Delta E^{(i)}/\Delta E^{(0)}$
1	$0.472127 \times 10^{-2}$	$0.120066 \times 10^{-1}$	$0.152015 \times 10^0$	$0.370934 \times 10^1$
2	$0.822788 \times 10^{-2}$	$0.122866 \times 10^{-2}$	$0.748139 \times 10^{-1}$	$0.266487 \times 10^1$
3	$0.736385 \times 10^{-3}$	$0.137055 \times 10^{-4}$	$0.202148 \times 10^{-1}$	$0.221931 \times 10^0$
4	$0.799667 \times 10^{-5}$	$0.168085 \times 10^{-8}$	$0.110762 \times 10^{-2}$	$0.711816 \times 10^{-3}$
5	$0.978799 \times 10^{-9}$	$0.252205 \times 10^{-16}$	$0.325281 \times 10^{-5}$	$0.615062 \times 10^{-8}$
6			$0.279782 \times 10^{-10}$	$0.454904 \times 10^{-18}$
	$\Delta E^{(0)} = 0.260572 \times 10^1$		$\Delta E^{(0)} = 0.751039 \times 10^2$	

$$\Delta F^{(i)} = {}^{t+\Delta t}R - {}^{t+\Delta t}F^{(i)}$$

$$\Delta E^{(i)} = \Delta F_x^{(i-1)} \Delta U_x^{(i)} + \Delta F_y^{(i-1)} \Delta U_y^{(i)}$$

$$F_{ref} = 2\sqrt{{}^1R_x^2 + {}^1R_y^2} = 4123.11$$

Graphical representation of solution is given in Fig. 3(b). From the positions of the stress points  $N'_1$  and  $N'_2$  in deviatoric plane we see that the loading is very nonradial. The points  $N''_1$  and  $N''_2$ , corresponding to the stress point  $N'_1$  and  $N'_2$ , are exactly on the yield curve.

## 5. Conclusion

An implicit scheme for stress integration of elastic-plastic constitutive relations, and calculation of elastic-plastic matrix – consistent with the stress integration procedure, represent an application of the governing parameter method (GPM) to the von Mises material with mixed hardening.

The presented procedure is simple and computationally efficient, suitable for general application in the displacement-based finite element method. The derived relations can be employed to 3-D, 2-D, plane stress/shell, beam and pipe conditions. The solved examples illustrate some of the main characteristics of the developed algorithm.

## REFERENCES

- [1] Kojić, M., *A general concept of implicit integration of constitutive relations for inelastic material deformation*, (in Serbian), Center for Scientific Research of Serbian Academy of Sciences and Arts and University of Kragujevac, Kragujevac, (1993).
- [2] Kojić, M., *Computational algorithms in inelastic analysis of solids and structures*, Oxford University Press, New York, in press.

- [3] Krieg, R.D., and Krieg, P.M., *Accuracies of numerical solution methods for the elastic-perfectly-plastic model*, ASME J. Press. Vess. Tech. 99 (1977), 510-515.
- [4] Ortiz, M., Pinsky, P.M., and Taylor, R.L., *Operator split methods for the numerical solution of the elastoplastic dynamic problem*, Comp. Meth. Appl. Mech. Engng., 39 (1983), 137-157.
- [5] Ortiz, M., and Simo, J.C., *An analysis of a new class of integration algorithms for elastoplastic constitutive relations*, Int. J. Num. Meth. Engng., 23, (1986), 353-366.
- [6] Kojić, M., and Bathe, K.J., *The "effective-stress-function" algorithm for thermo-elasto-plasticity and creep*, Int. J. Num. Meth. Engng., 24 (1987), 1509-1532.
- [7] Kojić, M., and Bathe, K.J., *Thermo-elastic-plastic and creep analysis of shell structures*, Comp. Structures, 26, No. 1/2, (1987), 135-143.
- [8] Kojić, M., Vukićević, M., and Slavković, R., *An implicit procedure for stress integration in elastic-plastic deformation of the modified Cam-clay material*, Proceeding of International Conference Complas III, Barcelona, (1992).
- [9] Kojić, M., *The effective-stress-function algorithm for von Mises anisotropic material*, Int. J. Num. Engng, in press.

L'INTÉGRATION IMPLICITE DE CONTRAINTE SE RAPPORTANT  
À LA DÉFORMATION  
ÉLASTO-PLASTIQUE DU MATÉRIAU AU RENFORCEMENT  
COMBINÉ DÉFINIE PAR VON MISES

La méthode du paramètre fondamentale est appliquée à l'intégration de contrainte dans le cas de la déformation élasto-plastique du matériau au renforcement combiné définie par la condition de fluage de von Mises. Ensuite, on détermine la contrainte d'incrément aux déformations déterminées dans le cas général de déformation 3-D aussi que dans des conditions de l'état plan de contrainte de coque et de poutre. Des expressions sont aussi déduites concernant la constitutive matrice élasto-plastique tangente.

Quelques exemples numériques illustrent l'efficacité et la simplicité du procédé numérique proposé.

IMPLICITNA INTEGRACIJA NAPONA  
U SLUČAJU ELASTIČNO-PLASTIČNE DEFORMACIJE  
FON MIZESOVOG MATERIJALA SA MEŠOVITIM OJAČANJEM

U radu se primenjuje metod osnovnog parametra na integraciju napona za elastično-plastično deformisanje metala definisano Mizesovim uslovom tečenja sa mešovitim ojačanjem. Izlaže se postupak određivanja napona u koraku pri zadatim deformacijama za opšti slučaj 3-D deformacije, kao i za uslove ravanskog stanja napona (ljuske) i greda. Izvode se takođe i izrazi za tangentnu elastično-plastičnu konstitutivnu matricu.

Na nekoliko numeričkih primera se ilustruje primena predloženog numeričkog efikasnog i jednostavnog postupka.

M. Kojić  
Mašinski fakultet  
ul. S. Janjića 6  
34000 Kragujevac, Jugoslavija